Capture vs Momentum and Kick and Correlation

D. Rubin

(Dated: August 25, 2021)

CONTENTS

Capture vs momentum and kick

For each muon that enters the ring, there is a range of kick angles that will lead to its capture. That kick angle capture range depends on the momentum of the muon and the angle and offset with which it exits the inflector. Since the closed orbit of the magic momentum muon is at the center of the aperture, the magic momentum muon it has the largest kick angle capture range, since it can tolerate the largest residual betatron oscillation amplitude. (For reference, the kick angle that directs the magic momentum muon with zero offset and zero angle onto its closed orbit is $\theta_k \sim 10.8$ mrad). The closed orbit for the muon with momentum offset $(\Delta p/p)_{max} = \eta/(45\text{ mm})$ is at the very edge of the aperture. The kick that steers the muon with that momentum offset $(\Delta p/p)_{max}$ onto its closed orbit, call it θ_k^{co}, is the only kick angle that leads to capture. If the kick is higher or lower than θ_k^{co}, the muon will oscillate about that orbit with a residual betatron amplitude, and thus be lost. It has zero tolerance for betatron oscillations. We see that in general the kick capture range shrinks with increasing (positive or negative) momentum offset.

The displacement of the particle from its closed orbit on exiting the inflector translates to an angle with which it crosses its closed orbit at the kicker. The angle of the trajectory exiting the inflector translates to a displacement at the kicker. Therefore, an angle at the inflector reduces the momentum acceptance. With a few simplifying assumptions, including continuous quads, and spatially uniform kicker field located $\phi = \pi/2$ downstream from the inflector exit, we can compute the kick angle capture range as a function of displacement and angle of trajectory exiting the inflector, and the particle momentum.

KICK VERSUS MOMENTUM

The radial closed orbit is given by $x_{co} = \eta\delta$ where δ is the fractional momentum offset, $\eta = R_0/(1-n)$ is the dispersion and $R_0 = 7.112$ is the magic radius. The muon oscillates about the closed orbit with some betatron amplitude $x_\beta(\phi)$, where ϕ is the betatron phase advance. Then

$$x(\phi) = \eta\delta + x_\beta(\phi)$$

where $\delta = \Delta p/p$. If $x_\beta(0) = x_0$ and $x'_\beta(0) = x'_0$ then

$$x_\beta(\phi) = x_0 \cos\phi + x'_0\beta \sin\phi \tag{1}$$

and

$$x'_\beta(\phi) = -\frac{x_0}{\beta}\sin\phi + x'_0\cos\phi \tag{2}$$

where $\beta = R_0/\sqrt{1-n}$. Then displacement from the magic radius is

$$x(\phi) = x_\beta(\phi) + \eta\delta = x_0\cos\phi + x_0'\beta\sin\phi + \eta\delta$$

At the inflector exit, the trajectory is displaced from the magic radius by x_{inf}. The center of the inflector aperture is displaced 77mm from the magic radius. The inflector aperture is ± 9 mm. Therefore 77-9 mm $< x_{inf} <$ 77+9 mm. Then at the inflector exit, where $\phi = 0$,

$$x(\phi = 0) = x_{inf} = \eta\delta + x_0 \rightarrow x_0 = x_{inf} - \eta\delta \tag{3}$$

The axis of the inflector is nominally parallel to the tanjent to the closed orbit of the magic momentum muon. Muons can exit the inflector with an angle x'_{inf} with respect to the axis.

The kicker is $\Delta\phi = \pi/2$ downstream from the inflector. The displacement at the kicker according to 1 is

$$x_k = \eta\delta + x_0'\beta.$$

The angle at the kicker

$$x_k' = -\frac{x_0}{\beta}$$

The kick compensates this angle. If the kick angle is (using 1)

$$\theta_k = -x_k' = \frac{x_0}{\beta} = \frac{x_{inf} - \eta\delta}{\beta} \tag{4}$$

and the inflector exit angle (x_0') is zero, then the particle is steered onto its closed orbit ($\Delta R = \eta\delta$). It is clear that high momentum particles require a smaller kick and low momentum particles a larger kick. Note that if $x'_{inf} \neq 0$, the trajectory is displaced from the closed orbit in the kicker and the best we can do is steer the particle onto a trajectory parallel to its closed orbit. The particle will oscillate about its closed orbit with amplitude equal to the residual displacement.

Substituting Equation 3 into Equations 1 and 2 the displacement and angle of the trajectory downstream from the inflector is

$$\begin{aligned} x(\phi) &= (x_{inf} - \eta\delta)\cos\phi + x'_{inf}\beta\sin\phi + \eta\delta \\ x'(\phi) &= -\frac{1}{\beta}(x_{inf} - \eta\delta)\sin\phi + x'_{inf}\cos\phi \end{aligned}$$

At the kicker, $\phi = \pi/2$, and including the kick angle

$$\begin{aligned} x_k &= x'_{inf}\beta + \eta\delta \\ x_k' &= -\frac{1}{\beta}(x_{inf} - \eta\delta) + \theta_k \end{aligned}$$

where θ_k is the angle change due to the kicker. Beyond the kicker the displacement is

$$x(\phi) = x'_{inf}\beta\cos(\phi - \phi_k) + (-\frac{1}{\beta}(x_{inf} - \eta\delta) + \theta_k)\beta\sin(\phi - \phi_k) + \eta\delta \tag{5}$$

The muon is stored as long as $|x(\phi)| < A$ where A is the radius of the collimators. For a particular set of initial conditions of x_{inf}, x'_{inf} and θ_k, we can determine the range of momentum that satisfy the inequality. Let's rewrite 5

$$\begin{aligned} x(\phi) &= x'_{inf}\beta\cos(\phi - \phi_k) + (-\frac{1}{\beta}(x_{inf} - \eta\delta) + \theta_k)\beta\sin(\phi - \phi_k) + \eta\delta \\ &= \left[(x'_{inf}\beta)^2 + (-\frac{1}{\beta}(x_{inf} - \eta\delta) + \theta_k)\beta)^2\right]^{1/2}\cos(\phi - \phi_k - \alpha) + \eta\delta \\ &= D\cos(\phi - \phi_k - \alpha) + \eta\delta \end{aligned}$$

where

$$\tan\alpha = \frac{-(x_{inf} - \eta\delta) + \beta\theta_k}{x'_{inf}\beta} \quad \text{and} \quad D = \left[(x'_{inf}\beta)^2 + (-\frac{1}{\beta}(x_{inf} - \eta\delta) + \theta_k)\beta)^2\right]^{1/2}$$

Then

$$\begin{aligned}
&|x(\phi)| < A \\
&\rightarrow -A < -D + \eta\delta, \quad D + \eta\delta < A \\
&\rightarrow -A - \eta\delta < -D, \quad \text{and} \quad D < A - \eta\delta.
\end{aligned} \tag{6}$$

Equations 6 imply

$$\begin{aligned}
D^2 &< (A \pm \eta\delta)^2 \\
(x'_{inf}\beta)^2 + (-\frac{1}{\beta}(x_{inf} - \eta\delta) + \theta_k)\beta)^2 &< A^2 + (\eta\delta)^2 \pm 2A\eta\delta \\
(x'_{inf}\beta)^2 + (-x_{inf} + \theta_k\beta)^2 + (\eta\delta)^2 + 2(-x_{inf} + \theta_k\beta)\eta\delta &< A^2 + (\eta\delta)^2 \pm 2A\eta\delta \\
(x'_{inf}\beta)^2 + (-x_{inf} + \theta_k\beta)^2 - 2(x_{inf} - \theta_k\beta)\eta\delta &< A^2 \pm 2A\eta\delta \\
(x'_{inf}\beta)^2 + (-x_{inf} + \theta_k\beta)^2 - 2(x_{inf} - \theta_k\beta \pm A)\eta\delta &< A^2 \\
\frac{A^2 - (x'_{inf}\beta)^2 - (-x_{inf} + \theta_k\beta)^2}{-2(x_{inf} - \theta_k\beta \pm A)} &> \eta\delta \\
\frac{A^2 - (x'_{inf}\beta)^2 - (-x_{inf} + \theta_k\beta)^2}{\mp 2(A \pm (x_{inf} - \theta_k\beta))} &> \eta\delta \\
\mp\frac{1}{2}\left(A \mp (x_{inf} - \theta_k\beta) - \frac{(x'_{inf}\beta)^2}{A \pm (x_{inf} - \theta_k\beta)}\right) &> \eta\delta \\
\rightarrow -\frac{1}{2}\left(A - (x_{inf} - \theta_k\beta) - \frac{(x'_{inf}\beta)^2}{A + (x_{inf} - \theta_k\beta)}\right) &< \eta\delta < \frac{1}{2}\left(A + (x_{inf} - \theta_k\beta) - \frac{(x'_{inf}\beta)^2}{A - (x_{inf} - \theta_k\beta)}\right)
\end{aligned} \tag{7}$$

Equation 7 defines the range of momenta that will be stored for a particular value of the kick angle θ_k.

The maximum momentum that can be stored is that momentum that minimizes the betatron amplitude (D). The minimum of D with respect to momentum obtains when

$$\begin{aligned}
\frac{dD}{d\delta} &= 0 \\
0 &= \frac{\eta\delta - x_{inf} + \theta_k\beta}{D} \\
\rightarrow \eta\delta &= x_{inf} - \theta_k\beta
\end{aligned} \tag{8}$$

Replace $\eta\delta$ with $\theta_k\beta$ in 7 using 8 and solve for θ_k.

Inflector exit angle zero

If the injection angle, $x'_{inf} = 0$ then

$$\begin{aligned}
\frac{1}{2}\left(A + (-x_{inf} + \theta_k\beta)\right) &< x_{inf} - \theta_k\beta < \frac{1}{2}\left(A - (-x_{inf} + \theta_k\beta)\right) \\
-\frac{1}{2}\left(A + (-x_{inf} + \theta_k\beta)\right) + x_{inf} &> \theta_k\beta > -\frac{1}{2}\left(A - (-x_{inf} + \theta_k\beta)\right) + x_{inf} \\
\frac{1}{2}\theta_k\beta &> -\frac{1}{2}(A - x_{inf}) \rightarrow \theta_k\beta > x_{inf} - A.
\end{aligned}$$

The minimum kick angle to store anything is $\theta_k = (x_{inf} - A)/\beta$.

Nonzero inflector exit angle

In general, including finite injection angle x'_{inf} 7 and 8 give

$$
\begin{aligned}
x_{inf} - \theta_k\beta &< \frac{1}{2}\left(A - (-x_{inf} + \theta_k\beta) - \frac{(x'_{inf}\beta)^2}{A - (x_{inf} - \theta_k\beta)}\right) \\
E &< \frac{1}{2}\left(A + E - \frac{(x'_{inf}\beta)^2}{A - E}\right) \\
E(A-E) &< \frac{1}{2}\left(A^2 - E^2 - (x'_{inf}\beta)^2\right) \\
-E^2 + 2EA &< A^2 - (x'_{inf}\beta)^2 \\
0 &< E^2 - 2EA + A^2 - (x'_{inf}\beta)^2 \\
E &= A \pm \frac{1}{2}\sqrt{4A^2 - 4(A^2 - (x'_{inf}\beta)^2)} \\
E &= A + |(x'_{inf}\beta)| \\
x_{inf} - \theta_k\beta &= A + |(x'_{inf}\beta)| \\
\theta_k\beta &> x_{inf} - (A + |x'_{inf}\beta|)
\end{aligned}
$$

The minimum kick required to store a muon increases with increasing injection angle.

Kick slice

The slice of momenta captured by a particular kick is defined by the inequalities 7. The width of the captured slice is the difference of the endpoints of the range.

$$
\Delta(\eta\delta) = A - (x'_{inf}\beta)^2\left(\frac{A}{A^2 - (x_{inf} - \theta_k\beta)^2}\right) \tag{9}
$$

The midpoint of the captured momentum range is half the sum of the endpoints.

$$
\langle\eta\delta\rangle = (x_{inf} - \theta_k\beta) - (x'_{inf}\beta)^2\left(\frac{x_{inf} - \theta_k\beta}{A^2 - (x_{inf} - \theta_k\beta)^2}\right) \tag{10}
$$

$$
= \frac{1}{2}(x_{inf} - \theta_k\beta)\left(1 - \frac{(x'_{inf}\beta)^2}{A^2 - (x_{inf} - \theta_k\beta)^2}\right) \tag{11}
$$

Kick limits

The width of the slice is necessarily positive. With that constraint Equation 9 implies the inequality

$$
\begin{aligned}
&A^2 - (x_{inf} - \theta_k\beta)^2 > (x'_{inf}\beta)^2 \\
&\quad\rightarrow (x_{inf} - \theta_K\beta) < \pm[A^2 - (x'_{inf}\beta)^2]^{1/2} \\
&\qquad\rightarrow \theta_K\beta < x_{inf} \pm [A^2 - (x'_{inf}\beta)^2]^{1/2}
\end{aligned}
\tag{12}
$$

$$
\tag{13}
$$

Summary

The kick angle determines the range of momenta captured and stored in the ring. Equation 9 gives the width of that range as a function of kick and the angle and offset of the particle at the inflector exit. The centerpoint of the range is given by Equation 11. Note that if $x'_{inf} = 0$, that the width of the range is independent of initial offset and kick angle, as long as the kick angle is within the range $-A < x_{inf} - \theta_k\beta < A$.

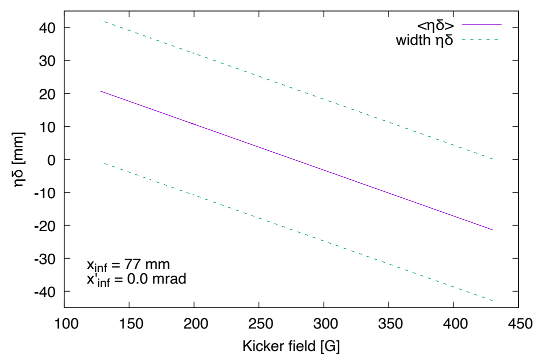

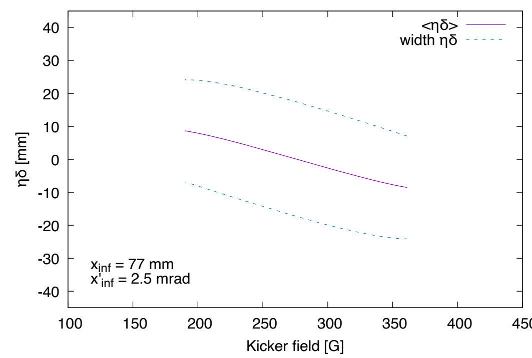

FIG. 1: Momentum acceptance as a function of kicker field, assuming $x'_{inf} = 0$ (left) and $x'_{inf} = 2.5$ mrad (right). All particle momenta between the dashed lines are stored. The solid line corresponds to the particle momentum (radial offset) that is kicked onto its closed orbit. The other momenta in the slice oscillate about their respective closed orbits with finite betatron amplitude. Note that the injection angle x'_{inf} reduces the momentum acceptance.

The minimum (and maximum) kicker field is determined by the ring parameters summarized in Table I. The range of momenta captured as a function of kicker field, assuming $x_{inf} = 77$mm is shown in Figure 1 (left) for $x'_{inf} = 0$ and 1(right) for $x'_{inf} = 2.5$mrad.

TABLE I

Parameter	Units	Value
field index (n)	-	0.11
$\beta = R/\sqrt{1-n}$	m	7.54
$\eta = R/(1-n)$	m	8.0
x_{inf}	m	0.077
A	m	0.043
$\theta_k^0 = x_{inf}/\beta$	mrad	10.2
θ_k^{min}	mrad	4.5
θ_k^{max}	mrad	15.9
B_k^0	G	276
B_k^{min}	G	121.8
B_k^{max}	G	430.2

The kicker pulse varies with time. A typical kicker pulse superimposed on the injected muon pulse is shown in Figure 2. The range of captured momenta and the midpoint of the momentum range will thus also vary with time according to Equations 11 and 9. The result is shown in Figure 3 for the kicker pulse in 2 assuming $x'_{inf} = 0$.

While the momentum range of captured particles is determined by the kicker field, the stored momentum distribution will depend on the momentum distribution of the injected beam. That distribution, according to simulation, is shown in Figure 4. The ring acceptance excludes all muons with momentum offset $|\eta\delta| > A \rightarrow |\delta| > 0.5375\%$.

The distribution of captured momenta in each time bin (as determined by the kick at that time), weighted by the intensity and momentum distribution of the injected muon pulse in that bin, is shown in Figure 5 for the case where the muons exit the center of the inflector aperture with zero angle and peak kicker field of 204 G. For the kicker field shown in 5(right), the momenta captured in each time bin corresponds to the error bar in 5(left). The average of the momentum and the average of the square of the momentum in each time bin assuming gaussian distributed momenta of the injected beam is shown in the right hand plot. Assuming the intensity distribution as shown in the right hand plot, we determine that the equilibrium radial offset of the distribution $\langle\eta\delta\rangle = 12.15$ mm with standard deviation $\sigma_r = 12.62$mm. For reference, recall that for Run I, with $B_{kicker} \sim 204G$ we measured average and width of the momentum distribution to be $\langle\eta\delta\rangle \sim 6$mm, and $\sigma_r \sim 9$mm respectively. We might increase the kicker field to reduce the average displacement. But with that increased field we will capture more lower momenta muons and thus increase the width.

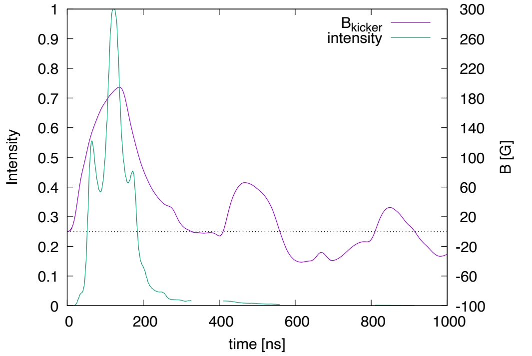

FIG. 2: The muon pulse (Run 1 T0 bunch 1) extends nearly 200 ns. The kicker pulse (Run 1 magnetometer measurement) is the purple curve. The peak of the kicker pulse is scaled to 204 G, typical in Run 1.

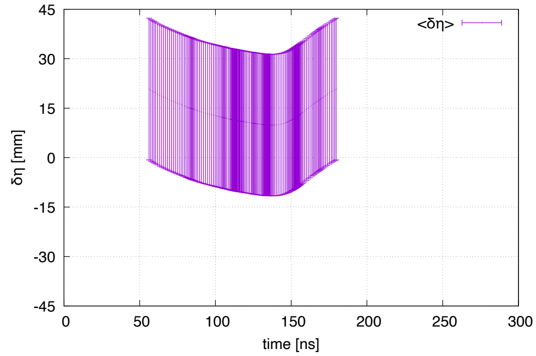

FIG. 3: The threshold kick angle for capture is $\theta_k = (x_{inf} - A)/\beta = 4.5$ mrad $\rightarrow 122$ G. The width of the range of captured momenta (the length of the error bar) is A/η. The midpoint of the range is $\langle \eta\delta \rangle = \frac{1}{2}(x_{inf} - \theta_k\beta)$. (The injection angle $x'_{inf} = 0$.

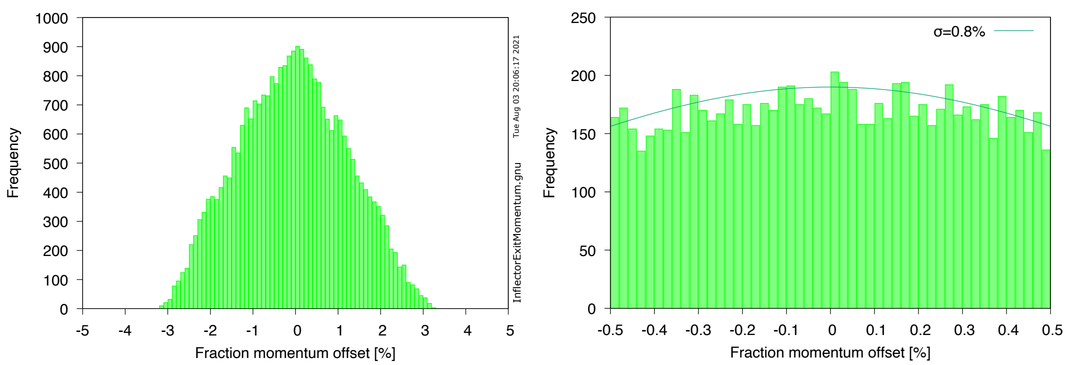

FIG. 4: Momentum distribution of all muons exiting the inflector (left). And those for which there are stable closed orbits in the storage ring (right). The shape of the distribution in the storable range corresponds (roughly) to a gaussian with $\sigma = 0.8\%$.

Correlation

The momentum-time correlation is evident. The highest average momenta are at the head and tail of the stored bunch where the kick is the weakest. The lowest average momenta corresponds to the peak of the kick. We might anticipate that with increasing peak kicker field, the variation of the momentum from head to tail of the bunch will also increase. The momenta at the head and tail will always be those picked up by the threshold kick, independent of the kick at the peak. Meanwhile, the momenta at the peak will decrease as the peak kick increases.

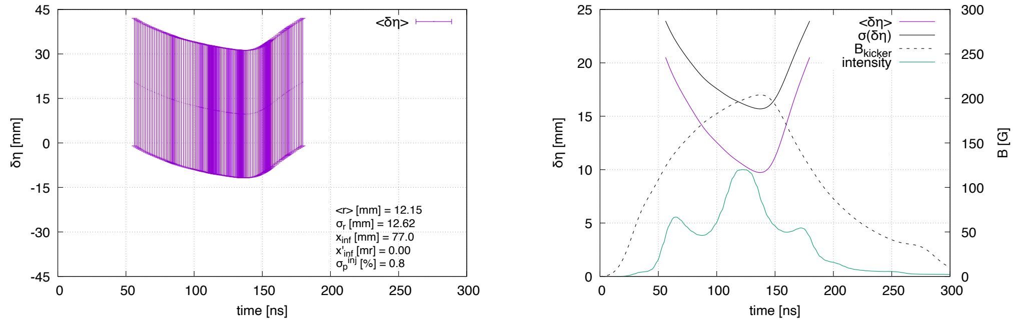

FIG. 5: Muons exit the center of the inflector aperture ($x_{inf} = 77$mm) with zero angle. The kicker field and muon intensity are shown at right. The peak kicker field is 204 G. The momentum bite ($\eta\delta_{max} - \eta\delta_{min}$), and the centroid of the bite captured in each time bin is shown at left. Note that in the case of $x'_{inf} = 0$ that the width of the momentum bite is independent of kick. The centroid decreases with increasing kick. The average momentum and the average of the square of the momenta in each time bin is shown at right. The average and standard deviation of momenta in the captured distribution, is $\langle\eta\delta\rangle = 12.15$ mm and $\sigma_r = 12.62$ mm.

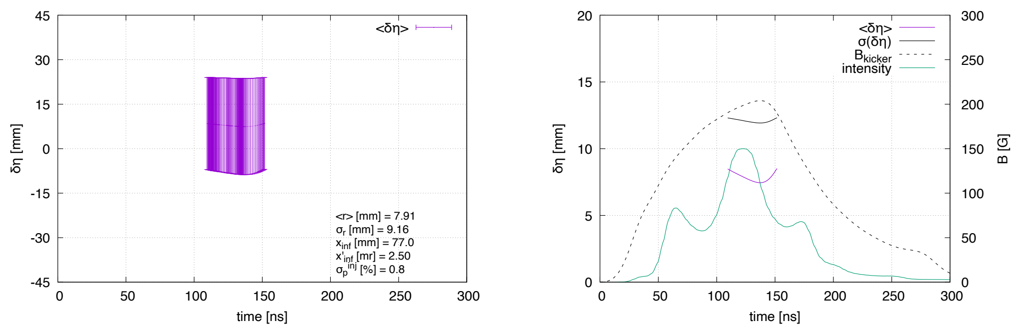

FIG. 6: Muons exit the center of the inflector aperture ($x_{inf} = 77$mm) with an angle $x'_{inf} = 2.5$ mrad. The kicker field and muon intensity is shown at right. The peak kicker field is 204 G. The momentum bite ($\eta\delta_{max} - \eta\delta_{min}$), and the centroid of the bite captured in each time bin is shown at left. The centroid decreases with increasing kick. The average momentum and the average of the square of the momenta in each time bin is shown at right. The average and standard deviation of momenta in the captured distribution, is $\langle\eta\delta\rangle = 7.91$ mm and $\sigma_r = 9.16$ mm.

Injection angle

As noted above, for trajectories that exit the inflector with nonzero angle, the momentum acceptance is reduced. Figure 6(left) shows the momentum bite captured in each time bin. The momentum acceptance is reduced as compared to the case with zero inflector angle, as is the length of the captured pulse and the momentum-time correlation.

Averaging over the injected distribution

In Figures 5 and 6 we show the momentum in the captured distribution based on Equations 9 and 11 for trajectories that exit the inflector with a unique offset and angle and a gaussian momentum distribution. Together they give the centroid and width of the momentum captured as a function of kicker strength. The distributions of the offset and angle of the injected beam are shown in Figure 7. The distributions are roughly gaussian and characterized by $\sigma_d = 3.5$mm and $\sigma_\theta = 2.6$ mrad respectively.

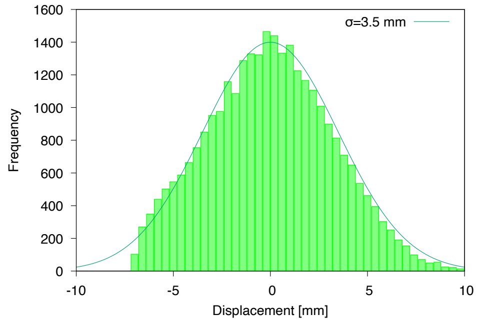

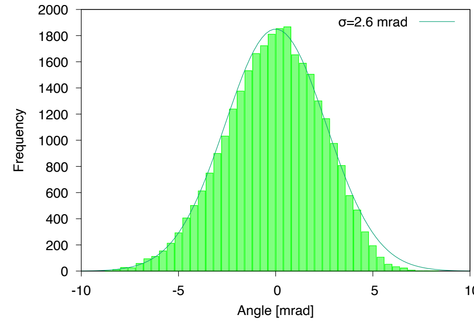

FIG. 7: Displacement(left) with respect to the center of the inflector aperture ($x_{inf} = 77$mm) and angle of the trajectory at the inflector exit as determined by simulation. Both distributions are roughly gaussian. The overlayed Gaussian curves have widths $\sigma_d \sim 3.5$mm and $\sigma_\theta \sim 2.6$ mrad respectively.

APPENDIX

Suppose a normal distribution of the momentum offset centered about zero.

$$\rho(\delta) = \frac{1}{\sigma\sqrt{2\pi}} e^{-\frac{1}{2}\left(\frac{\delta}{\sigma}\right)^2}$$

The average momentum for a particular kicker value is

$$\begin{aligned}
\langle\delta\rangle &= \left(\frac{1}{\int_{\delta_{min}}^{\delta_{max}} \rho(\delta) d\delta}\right) \int_{\delta_{min}}^{\delta_{max}} \delta\rho(\delta) d\delta \\
&= N(\delta_{max}, \delta_{min}) \int_{\delta_{min}}^{\delta_{max}} \delta \frac{1}{\sigma\sqrt{2\pi}} e^{-\frac{1}{2}\left(\frac{\delta}{\sigma}\right)^2} d\delta \\
&= N(\delta_{max}, \delta_{min}) \frac{1}{\sigma\sqrt{2\pi}} \int_{\delta_{min}}^{\delta_{max}} (-\sigma^2) \frac{d}{d\delta} \left(e^{-\frac{1}{2}\left(\frac{\delta}{\sigma}\right)^2}\right) d\delta \\
&= N(\delta_{max}, \delta_{min}) \frac{-\sigma}{\sqrt{2\pi}} \left(e^{-\frac{1}{2}\left(\frac{\delta}{\sigma}\right)^2}\right)_{\delta_{min}}^{\delta_{max}} \\
&= N(\delta_{max}, \delta_{min}) \frac{-\sigma}{\sqrt{2\pi}} \left(e^{-\frac{1}{2}\left(\frac{\delta_{max}}{\sigma}\right)^2} - e^{-\frac{1}{2}\left(\frac{\delta_{min}}{\sigma}\right)^2}\right)
\end{aligned}$$

The normalization

$$\begin{aligned}
\frac{1}{N(\delta_{max}, \delta_{min})} &= \int_{\delta_{min}}^{\delta_{max}} \frac{1}{\sigma\sqrt{2\pi}} e^{-\frac{1}{2}\left(\frac{\delta}{\sigma}\right)^2} d\delta \\
&= \int_{\frac{\delta_{min}}{\sqrt{2}\sigma}}^{\frac{\delta_{max}}{\sqrt{2}\sigma}} \frac{1}{\sigma\sqrt{2\pi}} e^{-t^2} \sqrt{2}\sigma dt \\
&= \frac{1}{\sqrt{\pi}} \frac{\sqrt{\pi}}{2} \left(\mathrm{erf}(\delta_{max}/(\sqrt{2}\sigma)) - \mathrm{erf}(\delta_{min}/(\sqrt{2}\sigma)\right)
\end{aligned}$$

The variance depends on

$$
\begin{aligned}
\langle\delta^2\rangle &= N(\delta_{max},\delta_{min})\int_{\delta_{min}}^{\delta_{max}}\delta^2\frac{1}{\sigma\sqrt{2\pi}}e^{-\frac{1}{2}\left(\frac{\delta}{\sigma}\right)^2}d\delta \\
&= N\frac{1}{\sigma\sqrt{2\pi}}\int_{\delta_{min}}^{\delta_{max}}\delta^2 e^{-\frac{1}{2}\left(\frac{\delta}{\sigma}\right)^2}d\delta \\
&= N\frac{1}{\sigma\sqrt{2\pi}}\int_{\delta_{min}}^{\delta_{max}}\sigma^2\left(-\frac{d}{d\delta}\left(\delta e^{-\frac{1}{2}\left(\frac{\delta}{\sigma}\right)^2}\right)d\delta + e^{-\frac{1}{2}\left(\frac{\delta}{\sigma}\right)^2}d\delta\right) \\
&= N\frac{1}{\sigma\sqrt{2\pi}}\left(-\sigma^2\delta e^{-\frac{1}{2}\left(\frac{\delta}{\sigma}\right)^2}\right)_{\delta_{min}}^{\delta_{max}} + \sigma^2 \\
&= N\frac{\sigma}{\sqrt{2\pi}}\left(-\delta e^{-\frac{1}{2}\left(\frac{\delta}{\sigma}\right)^2}\right)_{\delta_{min}}^{\delta_{max}} + \sigma^2
\end{aligned}
$$